Role of EPAC in axon determination

Munoz Llancao, Pablo Andrés

Chapter 6:

Microtobule-regulating proteins and cAMP-dependent signalling in neuroblastoma differentiation

Pablo Muñoz-Llancao, Cristian de Gregorio, Christopher Meinohl, Kevin Noorman, Erik Boddeke, Frank Lezoualc'h, Martina Schmidt, and Christian Gonzalez-Billault.

Microtobule-regulating proteins and cAMP-dependent signalling in neuroblastoma differentiation

Pablo Muñoz-Llancao[1, 2#], Cristian de Gregorio[1#], Christopher Meinohl[2], Kevin Noorman[2], Erik Boddeke[3], Frank Lezoualc'h[4, 5], Martina Schmidt[2, *] and Christian Gonzalez-Billault[1, *]

(1) Laboratory of Cell and Neuronal Dynamics, Department of Biology and Institute for Cell Dynamics and Biotechnology, Faculty of Sciences, Universidad de Chile, Santiago, Chile (2) Department of Molecular Pharmacology, University of Groningen, Groningen, The Netherlands. (3) Department of Medical Physiology, University Medical Center Groningen, University of Groningen, The Netherlands. (4) Inserm UMR-1048, Institut des Maladies Métaboliques et Cardiovasculaires, Toulouse, France, (5) Université de Toulouse III, Paul Sabatier, Toulouse, France.

(#) These authors equally contributed to this work

(*) Shared senior authorship; Corresponding authors

Christian Gonzalez-Billault PhD

Laboratory of Cell and Neuronal Dynamics (Cenedyn),

Department of Biology

Faculty of Sciences,

Universidad de Chile,

Las Palmeras 3425

780-0024, Santiago

Chile

Phone: 56 2 978 7442

Fax: 56 2 271 2983

Email: chrgonza@uchile.cl

Martina Schmidt

University Centre for Pharmacy

Antonius Deusinglaan 1

9713 AV Groningen, The Netherlands

m.schmidt@rug.nl

Phone: +31 50 363 3322

Fax: +31 50 363 6908

Abstract

Neurons are highly differentiated cells responsible for the conduction and transmission of information in the nervous system. The proper function of a neuron relies on the compartmentalization of their intracellular domains. Differentiated neuroblastoma cells are thoroughly used to study and understand the physiology and cell biology of neuronal cells. We showed that differentiation of N1E115 neuroblastoma cells is higher in the presence of a chemical analog of the cyclic AMP, (db-cAMP). We next analysed the expression of key microtubule regulating proteins in differentiated cells and the expression and activation of cAMP key players such as EPAC, PKA and AKAP79/150. Most of the microtubule-promoting factors were up regulated during differentiation of N1E-115 cells, while microtubule-destabilizing proteins were down-regulated. Moreover, we observed an increase in tubulin post-translational modifications related to microtubule stability. As expected, db-cAMP increased PKA and EPAC-dependent signalling. Consistently, pharmacological gain and loss function for EPAC-instructed cell differentiation, number of neurites, and neurite length in N1E-115 cells. Moreover, disruption of the PKA-AKAP interaction led reduced such morphometric parameters. Interestingly, PKA and EPAC act synergistically to induce neuronal differentiation in N1E-115. Altogether, these results show that the changes observed on the differentiation of N1E115 cells proceed by regulating some microtubule-stabilizing factors and the acquisition of a neuronal phenotype is a process involving concerted although independent functions of EPAC and PKA.

KEYWORDS

Neuronal differentiation, Cytoskeleton proteins, Microtubule-associated protein expression, cAMP, EPAC, PKA, Rap1.

Introduction

Neurons are highly polarized cells; they form two different functional domains, a single axon and multiple dendrites, which allows for the flow of information in the nervous system; Each domain is characterized by unique features that determine its molecular composition, maturation and functional properties (Banker and Cowan, 1977; Dotti et al., 1988). Studies conducted over the past 40 years regarding neuronal polarization have focused on understanding the sequential events that occur in primary neurons.

However, there is a complementary approach to understanding the phenomenon of neurite outgrowth based on the use of immortalized cell models. A major advantage that enables working with cell lines is that they are in constant division. This allows a large stock of cells to grow in short periods of time with the result of high levels of protein for experiments such as Western blots, immunoprecipitations, pull down assays, or gel electrophoresis 2-D. The possibility to perform transfection of genetic material, such as DNA or siRNA, with high transfection efficiencies, unlike neurons, which makes these cells useful for biochemical studies using genetic tools.

Several clonal cell lines have been used as models for neuronal differentiation under different treatments; the most studies use for instance, PC12, a rat adrenal pheochromocytoma cell line, that stops cell division and extend neurites in response to nerve growth factor (NGF) over a period of a week (Greene and Tischler, 1976). SH-SY5Y, a human neuroblastoma cell line, that under retinoic acid and brain-derived neurotrophic factor treatment produces cells with a cholinergic neuronal phenotype (Encinas et al., 2000). Neuro 2A

(N2A), a mouse neural crest-derived cell line that differentiates into a dopamine neuronal phenotype (Tremblay et al., 2010) and N1E-115, an adrenergic cell line derived from a mouse neuroblastoma, can both be differentiated into neuronal phenotype with cAMP analog such a dibutyryl-cAMP (Amano et al., 1972; Kato et al., 1982)

In the present study, we want to gain insight of N1E-115 neuronal differentiation induced by cAMP, since it has been shown that cAMP is essential in triggering the polarization of hippocampal neurons (Shelly et al., 2010). cAMP binds with similar affinity and directly activates protein kinase A (PKA) as well as the cAMP binding guanine nucleotide exchange factors; EPAC1 and EPAC2, and exchange factors for the small GTPases, Rap1 and Rap2, thereby activating both cAMP effectors (de Rooij et al., 1998; Dao et al., 2006). Previous studies characterized morphological and biochemical differences in N1E-115 cells, in response to serum deprivation and/or dimethylsulfoxide (DMSO) treatments (Reagan et al., 1990; Oh et al., 2006). However, the contribution of the cAMP-derived signalling pathways to N1E-115 is not fully addressed (de Rooij et al., 1998). Interestingly, previous work in neuroendocrine PC12 cells has suggested a role for EPAC and PKA in the transition from a proliferative into a non-proliferative neurite outgrowth-promoting signal (Kiermayer et al., 2005). Similarly, transient PKA activation triggers SH-SY5Y differentiation involving ERK and PI3K signalling (Sanchez et al., 2004).

In vivo, neural progenitor cells can differentiate into three different lineages: neurons, astrocytes, and oligodendrocytes (Luskin et al., 1993). Therefore, in order to distinguish amongst these cell populations, the

identification of specific subsets of molecular markers are required to evaluate neuronal differentiation (Kiermayer et al., 2005; Nakamuta et al., 2011b). Molecules that control microtubules and the actin dynamic are good markers for this phenomenon, since the cytoskeleton allows correct membrane trafficking and the delivery of specific proteins to their proper subcellular location such as axons and dendrites (Mandell and Banker, 1996; Gonzalez-Billault et al., 2001). Here, we evaluate changes in the microtubule cytoskeleton components of N1E-115 cells induced by cAMP-dependent differentiation, and assess the contribution of PKA and EPAC signalling during the acquisition of neuronal-like phenotypes.

Methods

Antibodies and chemicals

The following antibodies were used in this study: EPAC1 (immunofluorescence, 1:150, rabbit, Santa Cruz: H-70 sc-25632; Western blot, 1:300, mouse, Cell Signalling: 5B1 #4155), EPAC2 (immunofluorescence, 1:150, rabbit, Santa Cruz: H-220 sc-25633; Western blot, 1:300, mouse, Cell Signalling: 5D3 #4156), α-tubulin (1:10000, mouse, Sigma-Aldrich: #T6199), β-III-tubulin (Tuj1; 1:1000, mouse, Promega: #G1712A), Rap1 (1:300, rabbit, #sc-28197), Akap79 (1:300, Rabbit, Santa Cruz, sc-10764), PKA IIα reg (1:300, rabbit, Santa Cruz, sc-137220), PKA IIβ reg (1:300, rabbit, Santa Cruz, sc-25424), Phospho-CREB (Ser133) (1:300, Rabbit, Cell Signalling #S9191), MAP2 (1:500, rabbit, Millipore: AB5622), Tau1 (1:500, mouse, Millipore: MAB3420), Anti-Tyrosine tubulin (1:10000, Sigma), Anti-Acetylated tubulin (1:10000, Sigma), Anti-Detyrosinated tubulin (1:10000, Sigma) Anti SCG10-BR (1:1000, kindly provided by Dr Gabriela Grenningloh), Anti CRMP2 (1:1000, kindly provided by Dr. Kozo Kaibuchi; (Arimura et al., 2004)), Anti MAP1B (1:1000, N-19, Santa cruz), Anti MAP1A (1:1000, N-18, Santa cruz), Anti LIS1 (1:1000, H-300, Santa Cruz), phospho-PKA Substrate (1:1000, rabbit, Cell Signalling: 9624S), horseradish peroxidase (HRP)-conjugated anti–mouse IgG (1:5000, donkey, Jackson ImmunoResearch: #15-035-150), HRP-conjugated anti–rabbit [IgG (1:5000, donkey, Jackson ImmunoResearch: #711-035-152), Alexa Fluor® 488 Phalloidin, 1:500, Invitrogen, #A12379)

For immunofluorescence experiments, we used the following secondary antibodies: Alexa Fluor 488–conjugated anti–mouse IgG (1:600, donkey, Molecular Probes: #A21202), Alexa Fluor 546–conjugated anti–rabbit IgG (1:600, donkey, Molecular Probes: #A10040), Alexa Fluor 633-conjugated anti-rabbit IgG (1:500, Goat, Invitrogen, #A-21070)

Other reagents used include the following: DMSO (Sigma Aldrich, #472301), dibutyryl cAMP. (Db-cAMP; Sigma, #16980-89-5), retinoic acid (RA) (Sigma, #302-79-4), 8-pCPT-2'-*O*-Me-cAMP (8-pCPT; Biolog, #C041-05), InCELLect™ AKAP St-Ht31 Inhibitor Peptide (St-Ht31, Promega, #V8211), ESI-09 (Biolog, #B 133), ESI-05 (Biolog, #M092), CE3F4 (Frank Lezoualc'h, Université de Toulouse III, France), Lipofectamine 2000 (Invitrogen, #11668019), N^6- Benzoyladenosine- 3', 5'- cyclic monophosphate (6-Bnz-cAMP; Biolog, # B009-50), Protease Inhibitor Cocktail Tablets (Roche, #04693159001), Glutathione Sepharose 4B Media (Amersham, #17-0756-01), Western lightning plus-ECL (PerkinElmer, #NEL105001EA), Hoechst 33342 (1:10000, Invitrogen, #H3570), ROTI®-BLOCK (Carl Roth, #A151.2).

Animals

Adult C57Bl/6 wildtype mice were euthanized by with a lethal injection of Ketamine/Xylazine mix. The bioethical Committee of the Faculty of Sciences, University of Chile, approved all experiments according to the ethical rules of the Biosafety Policy Manual of the National Council for Scientific and technological Development (FONDECYT).

Cell culture

The neuroblastoma N1E115 cell line (Amano et al, 1971) was obtained from the American Type Culture Collection (ATCC, CRL-2263™). Cells were grown in complete DMEM medium (Gibco) containing 10% heat-inactive foetal bovine serum (FBS). Cell cultures were maintained at 37º C in a 95% humidified incubator with 5% CO2. To assay an effective method for N1E115 differentiation, the cells were grown in in normal DMEM medium with 10% FBS for 24 hours before stimulation with 10 mM retinoic acid (RA), 1,5% DMSO or 3 mM of dibutyryl cAMP.(Db-cAMP). The morphological changes of N1E115 were assessed after 3-5 days of differentiation induction.

Treatments

EPAC1 inhibition with CE3F4 (10 μM), EPAC2 inhibition with ESI-05 (15 μM), EPAC1/EPAC2 inhibition with ESI-09 (15 μM), AKAP-PKA interaction disruption with St-Ht31 (20 μM), EPAC activation with 8-pCPT (10 μM), and PKA activation with 6-BNZ-cAMP were performed on N1E-115 cultures at 24 h after plating. Briefly, all the compounds were dissolved in DMEM 0.5% medium in the presence or absence of 1mM of Db-cAMP, and incubated with the cultures for 3 days before inmmunostaining assays were carried out. The final DMSO concentration in all experiments was maintained below 0.1%.

RalGDS-GFP was kindly provided by Johannes Bos (University of Utrecht, Utrecht, The Netherlands). The transfection of N1E-115 cells using 4 μg of DNA/60-mm dish were performed with OptiMEM (Gibco) and Lipofectamine 2000 as directed by the manufacturer. The medium was changed after 6 h to fresh 0.5 % DMEM in presence of DMSO, Db-cAMP, and 8-pCPT. The cultures were

incubated for 3 days. All cultures were grown in a humidified culture incubator at 37°C, 5% CO_2.

Sample preparation and Western blot

N1E115 cells treated with DMSO or Db-cAMP, grown on dishes were washed once with PBS and then incubated with RIPA (65 mM Tris, 155 mM NaCl, 1% Triton X-100, 0.25% sodium deoxycholate, 1 mM EDTA, pH 7.4, and a mixture of protease inhibitors: 5 µg/ml Na_3VO_4, 20 µM PMSF, 5 mM NaF). Then, cells were scraped from the plate and kept on ice for 15 min and finally centrifuged for 20 min at 14,000 rpm. Supernatant fractions were denatured and subjected to SDS-PAGE, using 6% running gels for MAP1A, MAP1B, MAP2, AKAP79, 10% for EPAC, tyrosinated tubulin (Tyr Tub), detyrosinated tubulin (deTyr Tub), acetylated tubulin (Ac Tub), 15% for Rap1 and 12% for the PKA substrates, Tau, Phospho CREB, CRMP2, SCG10, and LIS. SeParated proteins were transferred to PVDF membrane, which were then blocked with 5% Roti Block for 1 h at room temperature. The membranes were incubated with primary antibodies overnight at 4°C. Membranes were then washed using TBST (50 mM Tris-HCl, 150 mM NaCl, 0.05% (w/v) Tween 20, pH 7.4) four times for 10 min each and incubated with HRP-conjugated secondary antibody for 1 h at room temperature. Finally, the membrane blots were developed using Western lightning plus-ECL. Digital images of Western blots were quantified using the ImageJ (NIH) software and the values are expressed as arbitrary units (a.u.).

GST fusion protein preparation and Rap1 activation pull-down assay.

Expression and purification of GST-conjugated proteins were performed as described (Henriquez et al., 2012). Briefly, BL21 (DE3) *E. coli* strains carrying

GST-RalGDS-RBD plasmid were grown overnight in LB medium containing ampicillin at 37°C. The next day, cultures were diluted 1:100 and grown in fresh medium until they reached an OD_{600} of 0.6. Then, 0.1 mM of isopropyl-β-D-thiogalactopyranoside (IPTG, final concentration) was added. Cells were collected and lysed 2 h after induction by sonication in lysis buffer A (50 mM Tris-HCl, pH 8.0; 1% Triton X-100; 1 mM EDTA; 0.15 M NaCl; 25 mM NaF; 0.5 mM PMSF; 1× protease inhibitor complex [Roche]). Cleared lysate was then incubated with glutathione-Sepharose beads (Amersham). Loaded beads were washed 10 times with lysis buffer B (lysis buffer A plus 300 mM NaCl) at 4°C. The GST fusion proteins were quantified and visualized in SDS-PAGE gels stained with Coomassie brilliant blue.

For the Rap1 activation assay, beads loaded with RalGDS-RBD (Rap-binding domain of the Ral guanine nucleotide dissociation stimulator, which binds specifically to Rap1-GTP but not to the inactive Rap1-GDP form) were incubated for 1 h at 4°C with 1 mg of freshly made lysate from 3-DIV N1E-115 cultures. Cell lysates were produced using fishing buffer (50 mM Tris-HCl, pH 7.5; 10% glycerol; 1% Triton X-100; 200 mM NaCl; 10 mM $MgCl_2$; 25 mM NaF; 1× protease inhibitor complex). The beads were washed three times with washing buffer (50 mM Tris-HCl, pH 7.5; 30 mM $MgCl_2$; 40 mM NaCl) and resuspended in SDS-PAGE sampling buffer. The levels of Rap1B-GTP (presented as arbitrary units) were evaluated from Western blot analysis and normalized against total Rap1B with ImageJ (values are presented as arbitrary units).

Immunofluorescence and image analysis

N1E-115 cells that were grown on coverslips were fixed at 72 h after transfection or pharmacological treatment with 4% (w/v) Paraformaldehyde/ 4% (w/v) sucrose for 30 min at 37°C and washed with phosphate-buffered saline (PBS) three times for 5 min each. The cells were incubated with PBS containing 0.1% Triton X-100 for 5 min and then blocked with 5% (w/v) bovine serum albumin (BSA) in PBS for 1 h. After blocking, cells were incubated with primary antibodies diluted with 1% BSA in PBS overnight at 4°C, washed with PBS three times for 5 min each, and incubated with fluorescent secondary antibody for 1 h and washed with PBS three times for 5 min each. Cells were incubated with antibodies against MAP2 (1:500), Tau (1:500), β-III Tubulin (Tuj1, 1:750), EPAC1 or EPAC2 (1:300) overnight at 4°C. Later, secondary antibodies were added and incubated for 1 h at room temperature. Cells were then washed 3 times with PBS 1X. Finally, coverslips were mounted on slides using FluorSave™ Reagent (Milipore, #345789) and examined using using a HC PL APO CS2 40x/1,3 (oil) objective on a Leica SP8 Confocal Microscope (DMI 600). ImageJ (NIH) software was used for the measure of neurite length, cell counting, and fluorescence intensity (The values are expressed as arbitrary units of the relative fluorescent of EPAC1 and EPAC2 to β–III tubulin). Phenotypes were determined by measuring neurite length and the number of neurites per cell. For the purposes of this study, we defined a differentiated cell as a cell with an neurite of >50 μm or more than twice the length of its soma. These experiments were

performed at the UMCG Microscopy and Imaging Center (UMIC), University of Groningen.

Statistical analysis

All data represent the mean ± s.e.m., of at least three independent experiments. Comparisons between two groups were made using the unpaired Student's t-test. Comparisons between three or more groups were performed using a one-way ANOVA followed by Dunnett's or Tukey's post hoc test. A value of $p < 0.05$ was considered significant. Analyses were performed with GraphPad Prism (GraphPad Software).

Results

Neuronal differentiation in N1E-115 cells is related to changes in the levels of microtubule associating and regulating proteins.

In the first set of experiments, we decided to analyse several inducers of neuronal differentiation. We analysed a range of concentration for each inducer and we established a working concentration based in the lowest amount to produce the differentiation of the N1E115 cells. The chosen amount for each inducer should also fulfil the condition of having been used in other cell lines system as a differentiation molecule. Based on these assumptions, we analysed the following compounds: DMSO, Retinoic Acid (RA) and dibutyryl-cyclic AMP (db-cAMP).

N1E115 cells were cultured for 24 hours and were then incubated in the differentiation-inducing agents for 5 days before fixation or protein extraction. Figure 1A shows representative images for each culture using different inducers. Undifferentiated N1E115 cells display a morphology characterized by rounded or polygonal cells without any cytoplasmic protrusion longer than one-cell body Figure 1A, (control panel). We next tested 10 mM retinoic acid and no changes were observed in the N1E115 cells, as indicated by the absence of prominent cell protrusions emerging from the cell body (Figure 1A, retinoic acid panel). DMSO was able to induce neuronal differentiation as shown in Figure 1A (DMSO panel). In this case, around 40% of cells displayed a differentiated morphology after 5 days in culture, characterized by the presence of neurites being at least two-cell bodies in length (Figure 1A, DMSO panel). In the case of 2 mM db-cAMP, most

of the cells were differentiated and displayed more than one protrusion longer than two-cell bodies emerging from the cell body (Figure 1A, Db-cAMP panel)

We analysed the percentage of differentiation for each treatment (Figure 1B). Db-cAMP was the most effective compound in inducing differentiation after 5 days, as indicated by the percentage of differentiated cells (80% against <40% in DMSO, < 10% in RA and <5% in control cells). These results confirm that increasing the levels of cAMP is the best method to induce differentiation in the N1E-115 cells (Liu et al., 1987). For the rest of the study, we set the Db-cAMP concentration at 1 mM, while DMSO was used as control condition.

Next, we evaluated the phenotype characteristics of differentiated N1E-115 cells by using the neuronal marker, β-III-Tubulin (Tuj1) that has been previously shown to increase its expression in differentiated N1E-115 cells (Oh et al., 2006). Figure 1C and Figure 1D show that 1mM of Db-cAMP is sufficient to induce a 77 ± 5% differentiation. Additionally, we analysed some morphometric parameters. Figure 1E shows that Db-cAMP increases the number of neurite-bearing cells (mean: Db-cAMP 3.4±0.31 vs DMSO 1.6±0.2 neurites). Moreover, we quantified the longest neurite length in the cells under the treatments. Figure 1F shows that DMSO treated cells present neurites with a length of 34.3±3 μm. In contrast, the longest neurite in cells treated with Db-cAMP was 137,3 ± 13,1 μm.

Neuronal differentiation is supported by dramatic changes affecting its cytoskeleton, both in primary neurons and neuroblastoma cell lines. Therefore, we decided to analyse several cytoskeleton components in detail, such as actin

microfilaments and post-translational modifications of tubulin. We used protein extracts derived from mouse brain as a positive control. Figure 1G shows the staining for both microtubules and actin microfilaments in undifferentiated and differentiated cells. Undifferentiated cells, as expected, displayed a rounded morphology, characterized by the presence of actin rich zones in the periphery of the cells, corresponding to filopodia and lamellipodia. In contrast, most of the microtubules were restricted to the cell body (Figure 1G, DMSO). In differentiated Db-cAMP cells, microtubules were distributed along the protrusive extension emerging from the cell bodies, while actin filaments were prominent in the distal tips of neurites forming growth cone-like structures and lamellipodia around cell body (Figure 1G, Db-cAMP). Interestingly, differentiated cells displayed an increased tyrosinated tubulin (Tyr Tub) at the distal part of the neurites, a feature that is related to highly dynamic microtubules and recapitulates what occurs during axon development in primary neuronal cells (Witte et al., 2008), (Figure 1G, insert). Such accumulation of tyrosinated microtubules was not accompanied by an overall change in the total amount of such tubulin post-translational modification (Figure 1H). In contrast, we found that the overall levels of detyrosinated (Figure 1I) and acetylated tubulin (Figure 1J) are higher in differentiated cells. Interestingly, these two posttranslational modifications have been linked to a pool of stable microtubules (Janke and Kneussel, 2010), which contribute to the axonal elongation (Witte et al., 2008).

The morphological changes described above should rely on the differential expression of cytoskeleton-regulating proteins. To test this hypothesis, we prepared cell extracts from non-differentiated and differentiated N1E115 cells.

We analysed a repertoire of microtubule-associated proteins that have been previously implicated in primary neuronal differentiation (Gonzalez-Billault et al., 2002; Conde and Caceres, 2009). Figure 2A shows the immunostaining of the microtubule-associated proteins (MAPs) MAP2 and Tau in differentiated cells along the longest neurite and cell body, showing no preferential subcellular localization. We quantified the fluorescence intensity for these proteins and found that both MAP2 and Tau are increased in differentiated cells (Figure 2B). We then evaluated changes in the overall amount of proteins through Western blotting. Figures 2C and 2D show that differentiated N1E115 cells displayed increased levels of MAP2 and Tau, that correlated with the observation in Figure 2A.

We next performed Western blot analysis of MAP1A and MAP1B, two MAPs that play a role in regulating the neuronal cytoskeleton; MAP1B during axon formation and MAP1A in maintenance of mature neurons morphology (Cravchik et al., 1994; Gonzalez-Billault et al., 2001). Our results in Figures 2E and 2F show statically significant differences between undifferentiated and differentiated cells for MAP1A and MAP1B. Overall, these results indicate that increased amounts of microtubule-associated proteins are needed to develop neurites in differentiated cells.

We also analysed other proteins that directly regulate microtubule stabilization, and therefore could also be implicated in N1E-115 differentiation. We focused our attention on the proteins LIS1 and CRMP2, which are two interesting microtubule stabilization and/or promoting factors (Conde and Caceres, 2009). LIS1 is a non-canonical microtubule associated protein that

plays a prominent role in microtubule advance during growth cone remodelling, a process in axonogenesis (Grabham et al., 2007) Figure 2G shows that no significant differences were found between the DMSO and Db-cAMP group. On the other hand, CRMP2 a protein that promotes the assembly of tubulin heterodimers enhancing microtubule-polymerization during axon formation (Fukata et al., 2002), was significantly increased in differentiated cells. (Figure 2H).

Finally, in this set of experiments, we wanted to determine whether the changes described in microtubule promoting proteins were accompanied by changes in microtubule destabilizing factors. We analysed the changes in the expression of SCG10, a protein that promotes disassembly of microtubules and is enriched in the growth cones of the developing neurons (Morii et al., 2006). Interestingly, the expression of SCG10 was decreased in N1E115 differentiated cells (Figure 2I). These results show that upon differentiation of N1E115 cells with Db-cAMP, a selective increase of posttranslational modification on tubulin, microtubule promoting factors, and decreases of proteins inducing microtubule disassembly was displayed.

Changes in the activity of the cAMP effector, EPAC and PKA, in N1E-115 differentiated cells.

Based on the changes in morphology and cytoskeleton composition described above, the next set of experiments were conducted to determine whether changes in cytoskeleton proteins described in the previous section were accompanied by changes in the cAMP effectors such as PKA and EPAC, since these proteins mediate the majority of effects of cAMP in mammalian cells

(Cheng et al., 2008). It has been previously suggested that EPAC proteins would be necessary to promote neuritogenesis in SH-SY5Y cells in a mechanism involving ERK activation (Birkeland et al., 2009). To determine which EPAC isoforms are expressed in N1E-115 cells, we first studied them by WWestern blotting the expression of EPAC1 and EPAC2. Figure 3A shows that both EPAC1 and EPAC2 are expressed in N1E-115 cells but their expression is not modified after Db-cAMP treatments.

Next, we evaluated the expression of the PKA type II regulatory subunit (i.e. RII α and RII β), because RIIs are the predominant PKA isoforms in the brain and RII is concentrated in the dendrites of cortical neurons (Cadd et al., 1990; Zhong et al., 2009). SH-SY5Y cells exposed to forskolin, a direct activator of adenylyl cyclase, resulted in a decrease of the levels of catalytic (C) and regulatory (RI and RII) PKA subunits. In contrast, a neuroblastoma-glioma-hybrid cell exposed to Db-cAMP does not change RI subunits (Lohmann et al., 1983). Moreover, our results in the previous section showed that Db-cAMP induces an increase in MAP2 protein, which is an anchoring protein for PKA in neurons by binding to RII PKA (Harada et al., 2002; Zhong et al., 2009). Figure 3B shows a significant increase in the levels of both PKA RIIs in differentiated cells, which suggests that in N1E-115 cells the regulatory mechanisms for PKA subunits due to increased cAMP may be different from other cell lines previously reported.

Since we found increased levels of RII β subunits (Figure 3B), we wanted to determine whether there could be a change in the expression of AKAP 79/150, because this AKAP contains a high-affinity binding site to the RII β and both

proteins are expressed in the brain in similar patterns of accumulation and localization (Glantz et al., 1992). In addition, EPAC2 interaction with AKAP79/150 regulates signalling cascades required for neuronal differentiation, such as PKB/Akt phosphorylation (Nijholt et al., 2008). Our results in Figure 3C show that AKAP79/150 is indeed expressed in N1E-115 cells, but with significantly decreased relative levels after Db-cAMP treatment.

We then decided to study signalling downstream from EPAC and PKA in order to further verify their activation during N1E-115 differentiation. In first term, we evaluated the activation of Rap1, a small GTPase activated by EPAC proteins. Figure 3D shows pull-down assays that specifically bind active Rap1 in N1E-115 cells treated with vehicle and Db-cAMP. Upon Db-cAMP treatment, Rap1 was significantly activated, confirming that EPAC increased expression, activating its canonical signalling pathway (Figure 3D). We also evaluated whether PKA was activated during Db-cAMP-dependent N1E-115 differentiation. We used two complementary strategies with phosphor-specific antibodies. We first evaluated changes in the immunodetection of whole protein extracts, using an antibody that specifically recognized phosphorylated-motifs by PKA. As indicated in Figure 3E, Db-cAMP treatment increased the amount of phosphorylated proteins by PKA (arrowheads). Similarly, CREB phosphorylation was also increased after Db-cAMP treatment, confirming that changes in the content of cAMP lead to increased PKA activity in N1E-15 cells (Figure 3F). All together, these results show for first time that EPAC1 and EPAC2 are expressed and active during N1E-115 differentiation. Furthermore, an increase of RII subunits might be related to higher activity of PKA under Db-cAMP treatment. Finally, the reduction of

AKAP79/150 levels does not seem to affect the catalytic activity of PKA.

Involvement of EPAC-Rap1 signalling in N1E-115 differentiation.

Having shown that Db-cAMP induced differentiation of N1E-115 cells, and that such a differentiation should be, in Part, linked to changes in EPAC and PKA signalling, we decided to further validate the role for EPACs in N1E-115 differentiation, as it has not been previously reported. First of all, we examined the subcellular distribution of EPAC1 (Figure 4A) and EPAC2 (Figure 4B) in differentiated N1E-115 cells. Our results show that both EPACs are concentrated in the cell soma in dB-cAMP group; but also that both EPACs are found in neurites, displaying a trend to accumulate toward the distal end of the neurites in the N1E-115 cells (Figure 4A and 4B, arrowheads).

To confirm that Db-cAMP was indeed activating the Rap1 protein, we transfected N1E-115 cells with a GFP-fused Ral-GDS-RBD construct, which is a reporter that has previously been used to assess subcellular localization of active Rap1 in several cell types (Bivona et al., 2004; Kortholt et al., 2010). Cells were transfected upon plating and further incubated with 1mM of Db-cAMP and the selective agonist of EPAC, 8-pCPT (10 μM) as a positive control. This was done until 3 DIV, when they were stained with Tuj1 to identify neurites (Figure 4D). We quantified the fluorescence intensity of Ral-GDS-GFP in the last third of each Tuj1-positive neurites for each treatment. Figure 4E shows that cells treated with Db-cAMP displayed increased Rap1 activity in their neurites. We then quantified immunofluorescence along the last 50 μm of each neurites and observed a preferential accumulation of active Rap1 at the distal end of neurites after Db-

cAMP treatment. Since 8-pCPT induced a similar response, our results suggest that increased EPAC levels activate Rap1 during neurite elongation of N1E-115 cells. These results are in line with previous results, showing the Participation of Rap1 during axon development in primary neurons (Schwamborn and Puschel, 2004).

EPAC and PKA independently regulate N1E-115 cell differentiation.

To further study the roles of EPAC and PKA in cAMP-induced neurite outgrowth, we used pharmacological tools to either increase or decrease EPAC and PKA signalling. We used the following reagents: an EPAC agonist termed 8-pCPT (10 μM) (Enserink et al., 2002), the PKA agonist, 6-Bnz-cAMP (6-Bnz) (10 μM) (Christensen et al., 2003), an EPAC1 selective inhibitor, CE3F4 (15 μM) (Courilleau et al., 2013), an EPAC2 selective inhibitor, ESI-05 (15 μM) (Tsalkova et al., 2012b; Almahariq et al., 2013), an EPAC1 and EPAC2 inhibitor, ESI-09 (10 μM)(Almahariq et al., 2013), and a membrane-permeable peptide that inhibits the interaction between RII PKA subunit and AKAPs, termed St-Ht31 (20 μM), (Schmidt et al., 2013; Poppinga et al., 2015). All working concentrations were determined based on previous works and in our laboratory determinations.

Figure 5A shows the phenotypic changes in the N1E-115 cells, under 8-pCPT and 6-Bnz treatments. In both cases, N1E-115 cells showed long cytoplasmic prolongations corresponding to neurites. We also combined both activators to examine a potential synergistic effect between EPAC and PKA during N1E-115 cell differentiation. We next evaluated morphometric Parameters such as percentage of cell differentiation (Figure 5B), number of neurites per cell

(Figure 5C), and average length of the longest neurite (Figure 5D). Both 8-pCPT and 6-Bnz significantly increased cell differentiation (8-pCPT: 65.4±1.5%, 6-Bnz: 68±6 %), whereas combined stimulation with 8-pCPT and 6-Bnz elicited an even higher effect (8-pCPT+6-Bnz: 85.2±4%). Analysis of the number of neurites showed that EPAC agonist, 8-pCPT increases the number of neurites comPared to the control (DMSO: 1.7±0.2 vs 8-pCPT: 2.6±0.2 neurites). Similarly, we found a significant increase on the number of neurites with 6-Bnz (2.3±0.2 neurites). Finally, 8-pCPT and 6-Bnz separately induced a significant increment of the longest neurite length (DMSO: 31.5±3.6 μm, 8-pCPT: 100.2±8.8 μm, 6-Bnz: 130±13 μm), although this effect was slightly higher with 6-Bnz. All in all, these results suggest that EPAC and PKA are acting in a synergistic manner to induce cell differentiation. It seems that EPAC most likely command the formation of new neurites, while EPAC and PKA would be responsible for neurite elongation.

In the last set of experiments, we sought to determine the role of specific EPAC isoforms on morphometrical changes induced by cAMP in N1E-115 cells. We performed pharmacological loss-of-function for EPAC1 and EPAC2 in the presence of Db-cAMP in order to rule out that PKA alone induces the changes observed during cell differentiation. We also evaluated AKAP function during N1E-114 differentiation. Figure 5D shows representative images of cells incubated with EPAC and AKAP inhibitors. All compounds used in this study were not deleterious at the concentrations selected, since no obvious morphological changes or compromised cell viability could be detected. We used cytoskeleton staining as well as Hoechst to evaluate cell integrity (not shown).

We then combined each inhibitor with Db-cAMP to evaluate potential reversion in the N1E-115 cell differentiation. Visual inspection suggests that every compound partially antagonized cell differentiation induced by Db-cAMP (Figure 5E). We then quantified the antagonists' effects. Amongst the antagonists tested, ESI-05 was the more efficient at reducing Db-cAMP-dependent differentiation of N1E-115 cells (DMSO: 17.4±2.3 %, CE3F4 + Db-cAMP: 66±2.4 %, ESI-05 + Db-cAMP: 20±3.5 %, ESI-09 + Db-cAMP: 58±3.7 %, St-Ht31 + Db-cAMP: 40±10.5 %, Db-cAMP: 84±3.0 %). Interestingly, ESI-09 treatment to inhibit both EPAC1 and EPAC2 did not cause an additive response, as we expected. Moreover, AKAP inhibition by St-Ht31 also reduced Db-cAMP-dependent differentiation. These results suggest that individual inhibition of EPAC isoforms affected cell differentiation and provide evidence that EPAC2 would be the main isoform to achieve differentiation in N1E-115 cells. Furthermore, the disruption of the association of RII-PKA with AKAPs suggests that such interaction is required to enhance N1E-115 differentiation.

We then analysed the number of neurites per cell (Figure 5G). We found that all compounds decreased the number of neurites per cell. (DMSO: 1.5±0.2, CE3F4 + Db-cAMP: 1.8±0.1, ESI-05 + Db-cAMP: 1.6±0.1, ESI-09 + Db-cAMP: 1.6±0.1, St-Ht31 + Db-cAMP: 1.9±0.2, neurites). Our results suggest that the outgrowth of new neurites during N1E-115 cell differentiation most likely relies on EPACs. Moreover, a proper subcellular localization of PKA is essential to generate new neurites and this localization should depend on AKAPs. Finally, we examined neurite elongation under these pharmacological conditions. As shown

in Figure 5H, EPAC1 and EPAC2 inhibition caused a significant reduction in the average length of the longest neurite. Similarly, AKAPS-PKA disruptors also induced a reduction in neurites length. (DMSO: 56±6.4 μm, CE3F4 + Db-cAMP:,100±8.2 μm, ESI-05 + Db-cAMP: 46±4.5 μm, ESI-09 + Db-cAMP: 92±10.3 μm, St-Ht31 + Db-cAMP: 55±4.8 μm, Db-cAMP: 163±12.4 μm). These data suggest that EPACs are necessary for both neurite outgrowth and elongation. Finally, it is suggested that appropriate subcellular localization of PKA –mediated by AKAP- contribute N1E-115 differentiation. The results presented here provide a molecular context that in part explains the effect of Db-cAMP upon neuroblastoma differentiation.

Discussion

Our current findings show that elevation of intracellular of cAMP induced the differentiation of N1E-115 cells, a process being accompanied by a series of changes on the levels of MAPs and cytoskeleton proteins. Furthermore, we show here for the first time, that differentiation of theN1E-115 cells by cAMP requires activation of EPACs and proper subcellular localization of PKA by AKAPs.

Previous studies showed that DMSO (Oh et al., 2005), RA (Oh et al., 2007) and serum withdrawal (Cosgrove and Cobbett, 1991) treatments elicited the neuronal differentiation of N1E-115 cells. Furthermore, N1E-115 cells differentiated with DMSO express several signalling proteins which include GTP-binding/Ras-related proteins, kinases, growth factors, calcium binding proteins, and phosphatase-related proteins). Such study suggested that a likely mechanism for DMSO effects could be related with the high abundance of retinoic acid binding proteins I and II (Busch et al., 1992; Oh et al., 2005). Interestingly; Clejan, et al.1996, showed that the differentiation of N1E-115 cells induced by DMSO was caused by inactivation of phospholipase D (PLD), along with activation of phospholipases C and of the sphingomyelin pathway (Clejan et al., 1996). It has also been shown that DMSO differentiation decreases cyclin dependent kinase (cdk) activities and phosphorylation of the retinoblastoma gene product (pRb) leading to neuronal differentiation (Kranenburg et al., 1995). All of these studies suggest that the mechanism undergo DMSO differentiation is independent of cAMP signalling and induced changes in cytoskeleton proteins. It has been shown that tubulin alpha-1 was highly expressed in differentiated cells. Unexpectedly, this study failed to report an increase of the neuronal tubulin

isotype beta III (Oh, et al., 2006). Serum deprivation and RA treatments in N1E-115 cells induced expression β-III-Tubulin, similar to this study (Oh et al., 2007). Changes in the amount of the enzyme tubulin tyrosine ligase (TTL), which is known to catalyse ligation of tyrosine residues to the COOH terminus of the detyrosinated form of alpha-tubulin, was observed in differentiated cells (Erck et al., 2005). Although our results did not show an increase in the overall tyrosination of microtubules, we detected accumulation of Tyr tubulin in the tips of the neurites, similar to what is observed in primary neurons (Utreras et al., 2008). Moreover, acetylated tubulin is increased during N1E-115 differentiation, (which may stimulate intracellular dynamics and cargo distribution as described in neurons (Janke and Kneussel, 2010). Finally, increased levels of detyrosinated tubulin, enriched in neurites from neuroblastoma cells, reproduce what is observed in axons (Shea et al., 1990; Janke and Kneussel, 2010). It may therefore be possible that different inductors activate redundant and differential molecular programs involved in tubulin expression during neuronal differentiation. MAPs are key factors involved in microtubule stabilization (Witte et al., 2008). In line with this, our findings indicate that, N1E-115 requires the expression of both dendritic and axonal MAPs. It has been described that in neurons MAPs display redundant functions (DiTella et al., 1996), while other studies suggest that MAPs can act synergistically (Gonzalez-Billault et al., 2002). One interesting feature derived from this work is the fact that MAP expression in differentiated N1E-115 cannot reproduce differential temporal and spatial patterns observed for the same subset of MAPs in primary neurons. MAP1A and MAP1B are similarly expressed in neuroblastoma cells, while the MAP2 and tau segregation observed

in primary neurons is not reproduced in N1E-115 differentiated cells. Increased MAP expression was not a general mechanism, since LIS1 levels were unchanged during differentiation. LIS1 promotes microtubule polymerization and is involved in growth cone remodelling (Grabham et al., 2007); however, it has not been directly involved in neuritogenesis (Bielas et al., 2004). Consistently with our findings, differentiation of SH-SY5Y cells by RA decreases LIS1 expression, reinforcing the idea that LIS1 functions seem to be dispensable for neurite outgrowth (Messi et al., 2008). CRMP2 is a protein that binds tubulin heterodimers, and is a molecular determinant of axon identity (Inagaki et al., 2001). Our results suggest that Db-cAMP induced such dramatic morphological changes, in part, by favouring the incorporation of soluble tubulin heterodimers into growing microtubule in neurites. Finally, SCG10, a neuronal member of the stathmin family, enhances microtubule dynamics during neuronal differentiation (Morii et al., 2006). Our results, suggest that Db-cAMP induced differentiation decreases the expression of proteins that does not favour microtubule elongation.

cAMP had been proposed as a key cytoplasmic factor involved in axonal outgrowth. For this reason, we studied the cross talk between cAMP/PKA- and cAMP/EPAC-dependent pathways. First, PKA regulates neuronal polarity by two mechanisms. PKA phosphorylates Smurf1 in response to brain-derived neurotrophic factor (BDNF), reducing the degradation of Par6—a member of the polarity complex-and enhancing the degradation of the small GTPase RhoA, which is an axonal growth-inhibitor protein and phosphorylating the protein LKB1 (Cheng et al., 2011a). The inhibition of RhoA has also been involved in N1E-115

cell differentiation (Marler et al., 2005), suggesting conserved molecular mechanisms. The role of PKA in neuroblastoma differentiation has been well studied in different cell lines. particularly, the RI subunit is increased in N1E-115 during treatment by Db-cAMP. However, such increase is not linked to neurite outgrowth (Liu et al., 1987). In this study, we found that both RII subunits increased during N1E-115 neuronal cell differentiation, suggesting a role of RII in neuritogenesis. PKA activity is required to promote differentiation of SH-SY5Y (Sanchez et al., 2004). Our data suggest that PKA may be involved in both neurite outgrowth and elongation. Since MAP2 expression is increased in N1E-115, it is likely that MAP2 can enhance PKA activation by interacting with the RII subunit of PKA promoting neurite elongation (Huang et al., 2013). Such regulation may, in turn, promote differential phosphorylation of MAPs such as tau and MAP2, leading to microtubule stabilization (Harada et al., 2002).

EPAC1 and EPAC2 bind cAMP with similar affinity as the PKA holoenzyme, suggesting that both factors may respond to similar cAMP physiological concentrations (Dao et al., 2006). The concerted functions of EPAC and PKA signalling are dependent on cellular context and processes (Grandoch et al., 2010a). Activation of the EPAC-dependent pathway may target several molecules that regulate axon formation and elongation such as Rap1 (Schwamborn and Puschel, 2004), c-Jun N-terminal kinase (JNK) (Hochbaum et al., 2003), the small GTPase, Rit, (Shi et al., 2006) and the small GTPases, Ras (Li et al., 2006) and Rho (Moon et al., 2013). Our data show that both isoforms of EPAC are expressed in N1E-115 cells; and to our understanding, this is the first evidence that shows the expression and subcellular distribution of these

signalling molecules in N1E-115 differentiating cells. Such EPAC induction was paralleled by increased Rap1 activity, suggesting that a spatial and temporal regulation of EPAC-Rap1 signalling is required to promote neurite outgrowth and extension. Noteworthy, such spatio-temporal regulation for EPAC-Rap1 axis is observed in primary neurons and determines the development of neuronal polarity (Schwamborn and Puschel, 2004; Muñoz-Llancao P, 2015). Using selective pharmacological inhibitors, we assessed the contribution of EPAC1 and EPAC2. Our results show that EPAC2, and to a lesser extent, EPAC1 are important in promoting neurite elongation. Similar results have been reported in rat dorsal root ganglion (DRG) neurons, through gain-of-function experiments using 8-pCPT and loss-of-function experiments using siRNA knockdown strategies to target both EPAC. Both experimental paradigms significantly affected neurite outgrowth in vitro (Murray and Shewan, 2008). Moreover, EPAC2 knockdown in cortical neurons *in vivo* and *in vitro* reduced basal dendritic architecture (Srivastava et al., 2012).

Finally, we investigated the role of AKAP79/150 in N1E-115 cell differentiation by cAMP. Noteworthy, it has been shown that in primary cortical neurons and HT-4 neuroblastoma cell lines, the A-kinase anchoring protein150 (AKAP150) may acts as a key regulator between the two cAMP signalling pathways (Nijholt et al., 2008). Our data show that the expression of AKAP79/150 is reduced during differentiation. Previous studies reported AKAP150 in primary branches of dendrites, where it is associated with microtubules (Glantz et al., 1992), and suggest that AKAP 79/150 loss causes an exclusion of the PKA holoenzyme from hippocampal dendritic spines, affecting

synaptic transmission (Tunquist et al., 2008). Our data showed that a relative reduction of AKAP150/79 did not impact neurite development induced by Db-cAMP. However, AKAP-PKA anchorage inhibitory peptide St-Ht31 led to a reduction in differentiation, number of neurites, and neurite length. These results suggest that PKA subcellular anchoring to other redundant AKAP could be necessary to induce neurite outgrowth. The importance of a proper PKA anchoring site may be relevant for the inhibition of RhoA by PKA. Previous studies revealed that PKA anchorage was necessary for the kinase to exert its inhibitory effect on RhoA activation and RhoA-dependent biological activities (Wang et al., 2006) and the phosphorylation of RhoA by PKA led this protein to degradation in hippocampal neurons inducing axon formation (Cheng et al., 2011a).

In conclusion, our results presented here indicate that Db-cAMP activates a molecular program in N1E-115 cells, leading to neurite outgrowth and elongation. This program involves changes of cytoskeleton proteins, including tubulin isotypes, tubulin post-translational modifications and MAPs. The cAMP signal was conveyed by EPAC and PKA effectors acting through independent but synergistic mechanisms, targeting the small GTPase, Rap1; and requiring a proper subcellular localization of PKA by AKAPs.

Figures legends

Figure 1. Db-cAMP induces efficient N1E-115 differentiation involving changes in microtubule properties

(A) N1E-115 differentiated cells stained with α-tubulin antibody for the identification of the neuronal cell phenotype. Cultured N1E115 cells grown for 5 days. Control medium (DMEM with 0.5% FBS), 10 mM retinoic acid (RA), vehicle (1.5% DMSO), and 2 mM db-cAMP. (B) Quantitation of differentiated cells was defined as cells that extended neurites of length equal to or greater than two times the diameter of the cell body (about 20 μm), 100 cells per conditions were quantified (C) Immunofluorescence of undifferentiated cells (DMSO, upper panel) and differentiated cells (1mM, Db-cAMP, lower panel) after 3 days in culture, stained with the neuronal marker, β-III-tubulin (Red) and Alexa488-phalloidin (Green). During differentiation, the cells develop primary and secondary neurite branches, and increased neurite outgrowth. (D) Quantification of the percentage of differentiated and undifferentiated cells in each treatment (n=126-151 cells, student's t-test, $p<0.05$; DMSO and Db-cAMP: differentiated vs undifferentiated, four independent experiments). (E) Number of neurites per cell in control and Db-cAMP treated cells (n=126 cells, student's t-test, $p<0.05$, four independent experiments). (F) Length of the longest neurite in control and Db-cAMP treated cells (n=126 cells, student's t-test, $p<0.05$, four independent experiments). (G) Differentiated cells displayed α-tubulin tyrosination (red) at the distal end of neurites (insert, arrowhead). (H) Western blot and quantification for Tyrosinated tubulin (Tyr Tub. Student's t-test, $p<0.05$, three independent experiments). (I)

Western blot and quantification for Detyrosinated tubulin (deTyr Tub. Student's t-test, $p<0.05$, three independent experiments). (J) Western blot and quantification for Acetylated tubulin (Ac Tub. Student's t-test, $p<0.05$, three independent experiments) Data represent the mean ± s.e.m.; n.s., not significant; *$p < 0.05$; ***$p < 0.001$. Scale bars: 20 μm in A, 50 μm in C, 20 μm in G. Brain lysate was used as positive control in Western blot assays.

Figure 2: Db-cAMP regulates the expression of proteins involved in microtubule dynamics regulation.

(A) Immunofluorescence of undifferentiated cells (DMSO, upper panel) and differentiated cells (Db-cAMP, lower panel) after 3 days in culture, stained with MAP2 (Red) and Tau-1 (Green) antibodies. Differentiated cells were positive for both neuronal MAPs. (B) Quantitative immunofluorescence analysis for MAP2 and Tau expression in undifferentiated and differentiated cells (n= 50 cells, student's t-test, $p<0.05$, three independent experiments).

Western blot assays show changes in the expression levels of MAPs proteins; MAP2 (C), Tau (D) MAP1A (E), MA1B (F), during N1E-115 differentiation (student's t-test, $p<0.05$, three independent experiments). Neuronal MAPs expression is increased during N1E-115 differentiation. Western blot assays showed no changes in the expression levels of LIS1 (G) and an increase in the expression of CRMP-2 levels (H). In contrast, Db-cAMP decreases the expression of the microtubule-depolymerizing factor SCG10 Data represent the mean ± s.e.m. ; n.s., not significant; *$p < 0.05$; **$p < 0.01$. Scale bars: 50 μm in A. Brain lysate was used as positive control in Western blot assays.

Figure 3. Changes in cAMP-dependent effectors during N1E-115 differentiation.

N1E-115 protein extracts derived from control and Db-cAMP treated cells were analysed. *n*=3 samples/treatment. (A) Western blot analysis reveals no significant changes in the expression of EPAC1 and EPAC2 after stimulation with Db-cAMP, (B) whereas the expression PKA RIIα and PKA RIIβ subunit was increase during differentiation. (C) AKAP79/150 expression was decreased during N1E-115 differentiation. (D) Rap1 activity is increased during N1E-115 differentiation. Active Rap1B was normalized against total Rap1B protein. (E-F) Changes in the activity of PKA were assessed by analysing immunopositive reaction against an antibody that recognizes PKA-specific phosphorylation epitopes (E) and CREB phosphorylation (F) after 3 days of stimulation of the N1E115 cells with Db-cAMP. PKA and EPAC signalling are increased in N1E-115 cells. Data are presented as means ± SEM (EPAC1: n = 12; EPAC2: n = 9; PKA RIIα: n = 3; PKA RIIβ n = 6; AKAP79: n = 7; Rap1-GTP: n = 6; phospho-PKA substrate: n = 9; phosphor-CREB: n = 4, student's t-test, n.s., not significant; *p < 0.05)

Figure 4. Activation of EPAC-Rap1 signalling during N1E115 neuronal differentiation.

Cells were immunostained with Tuj1 (red) and EPAC1 (A) and EPAC2 (B) (green) antibodies. Subcellular distribution for EPACs is indicated toward the distal end of neurites in differentiated N1E-115 (arrowheads). (C) Quantitative fluorescence for EPAC1 and EPAC2 normalized against tubulin, along neurites in

differentiated and undifferentiated cells (n=40 cells, student's t-tests, $p<0.05$, three independent experiments). (D) EPAC pharmacological activation by Db-cAMP and 8-pCPT induced Rap1 activation and accumulation toward the distal end of neurites. N1E-115 cells were transfected with the RalGDS-GFP construct, that specifically bind Rap1-GTP, and treated with DMSO, Db-cAMP or 8-pCPT and stained for Tuj1. RalGDS-GFP fluorescence intensity was colour-coded. Insert and arrowheads indicates region of high Rap1 activity in neurites from N1E-115 differentiated cells. (E) Quantitative analysis of GFP fluorescence in Tuj1-positives neurites (n = 11-23 cells, student's t-tests, three independent experiments). (F) Intensity plot profile for RalGDS-GFP distribution of cells shown in (D) along 50 μm of neurites. The profile shows activation of Rap1 in the distal end of the neurites treated with Db-cAMP (red trace) and 8-pCPT (green trace) as compared to control condition (black trace) (n=5 cells per treatment). Data represent the mean ± s.e.m.; n.s., not significant; *$p < 0.05$; **$p < 0.01$. Scale bars: 50 μm in A, B and D.

Figure 5. Pharmacological modulation of cAMP dependent pathways during N1E-115 differentiation.

(A) N1E-115 cells were treated with control vehicle, EPAC agonist (8-pCPT), PKA agonist (6-Bnz), and the combination of both (8-pCPT + 6-Bnz), and then were immunostained for Tuj1 (red) and Hoechst for nucleus. (B-D) Quantitative analysis of N1E-115 cells treated as in (A) shows the percentage of differentiated cells per condition (B), number of neurites (C), and length of the longest neurite (D) shows that the combination of both agonist enhanced cell differentiation (n = 20-40 cells, *$p < 0.05$; ****$p < 0.0001$ compare to DMSO, ### $p < 0.001$; 8-pCPT

vs 8-pCPT + 6-Bnz, &&p < 0.001; 6-Bnz vs 8-pCPT + 6-Bnz, one-way ANOVA with Tukey's post hoc test; three independent experiments). (D) N1E-115 cells were treated with control vehicle and the antagonist for EPAC1 (CE3F4), EPAC2 (ESI-05), both EPACs (ESI-09) and AKAP-PKA disruptor (St-Ht31), then immunostained for Tuj1 (red) and Hoechst for nucleus. Treatments did not induce any evident morphological changes amongst cells. (E) N1E-115 cells were differentiated with Db-cAMP in the presence of antagonist described in (D). (F-H) Quantitative analysis for N1E-115 differentiation induced by Db-cAMP in the presence of EPACs and AKAP inhibitors. Differentiated cells were evaluated for percentage of differentiated cells (F), number of neurites per cell (G), and the length of the longest neurite (H). (n = 20 cells, *p<0.05; ****p<0.0001 compare to DMSO, ##p<0.01; ####p< 0.0001 compare Db-cAMP, one-way ANOVA with Tukey's post hoc test; three independent experiments). Data represent the mean ± s.e.m.; n.s., not significant; Scale bars: 50 μm in A, D and E.

Figures

Figure 1

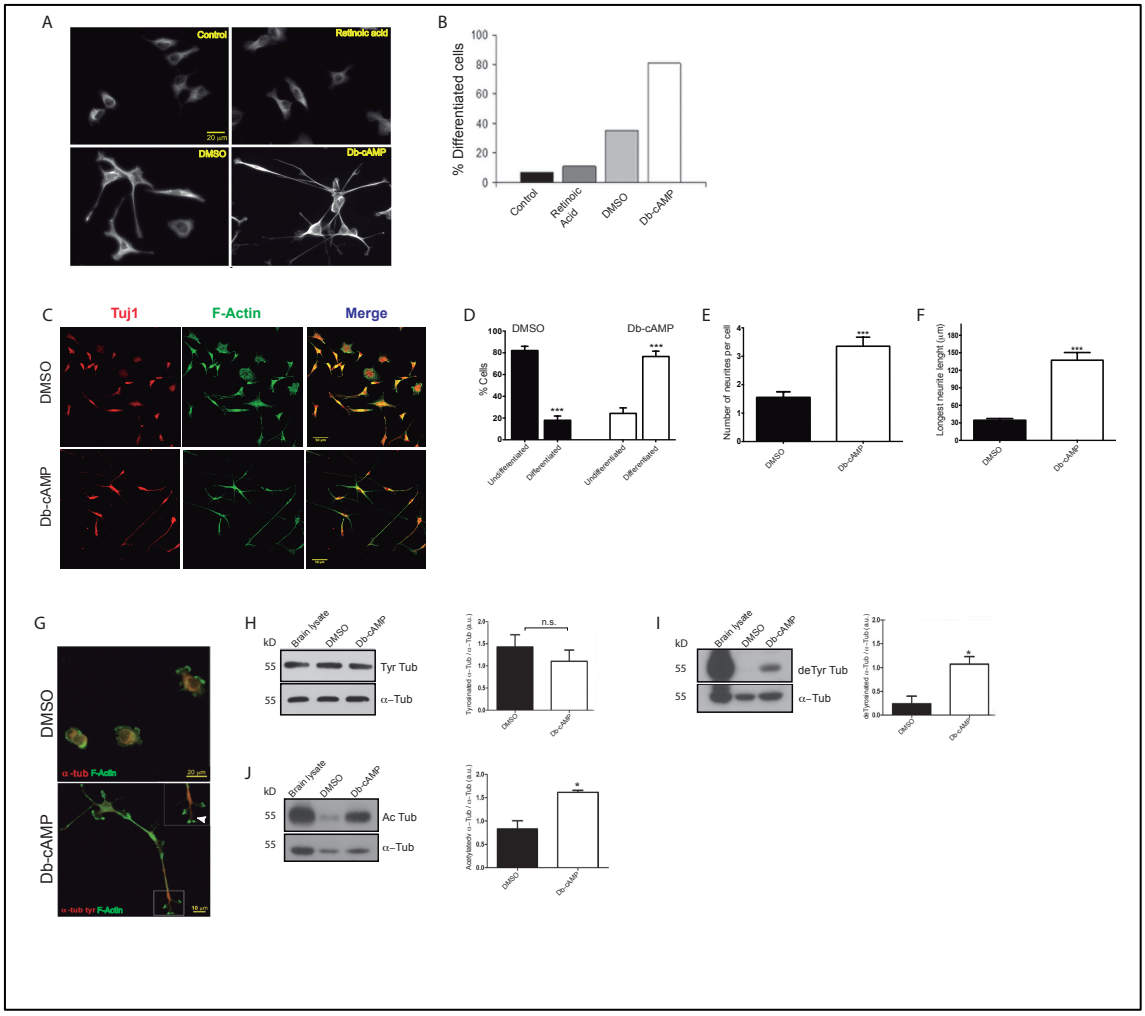

Figure 2

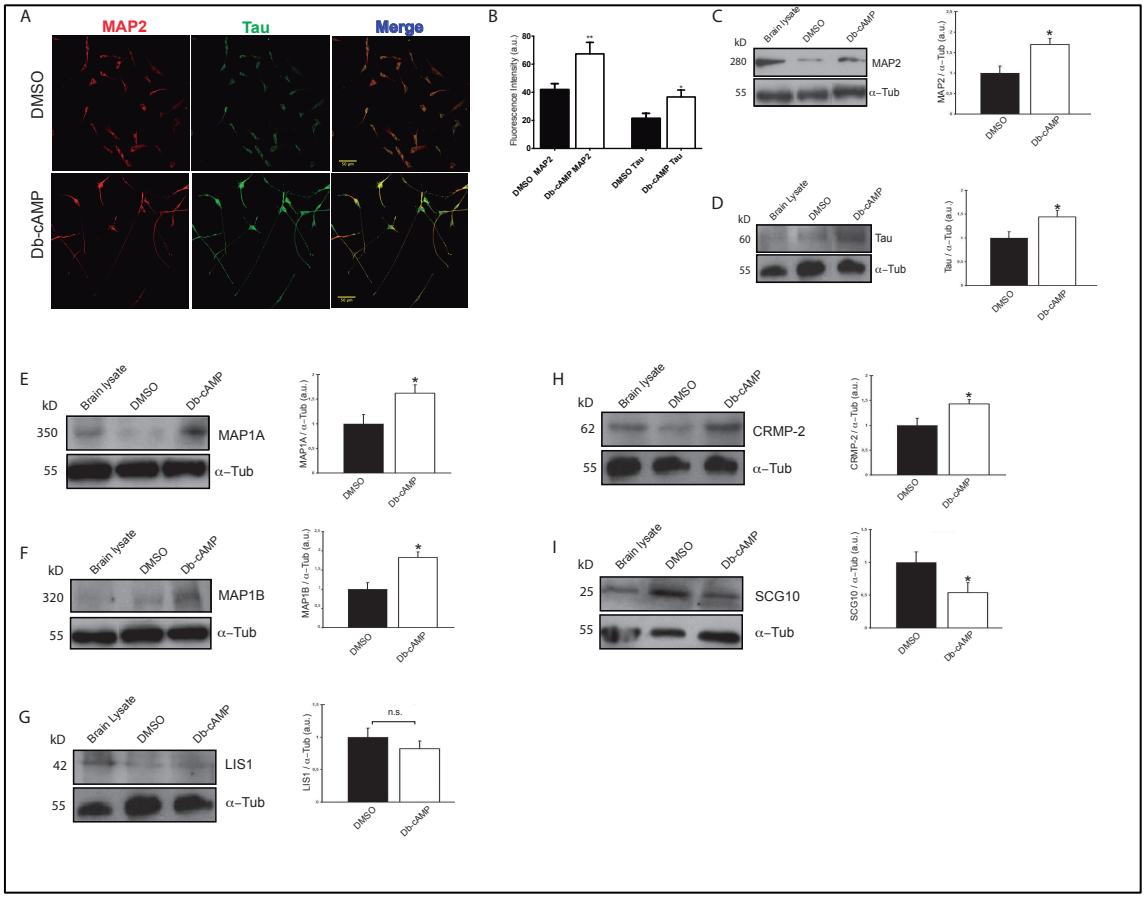
A
MAP2
Tau
Merge
DMSO
Db-cAMP
B
Fluorescence Intensity (a.u.)
DMSO MAP2
Db-cAMP MAP2
DMSO Tau
Db-cAMP Tau
C
Brain lysate
DMSO
Db-cAMP
kD
280
55
MAP2
α–Tub
MAP2 / α–Tub (a.u.)
D
60
55
Tau
α–Tub
Tau / α–Tub (a.u.)
E
350
MAP1A
MAP1A / α–Tub (a.u.)
F
320
MAP1B
MAP1B / α–Tub (a.u.)
G
42
LIS1
n.s.
LIS1 / α–Tub (a.u.)
H
62
CRMP-2
CRMP-2 / α–Tub (a.u.)
I
25
SCG10
SCG10 / α–Tub (a.u.)

Figure 3

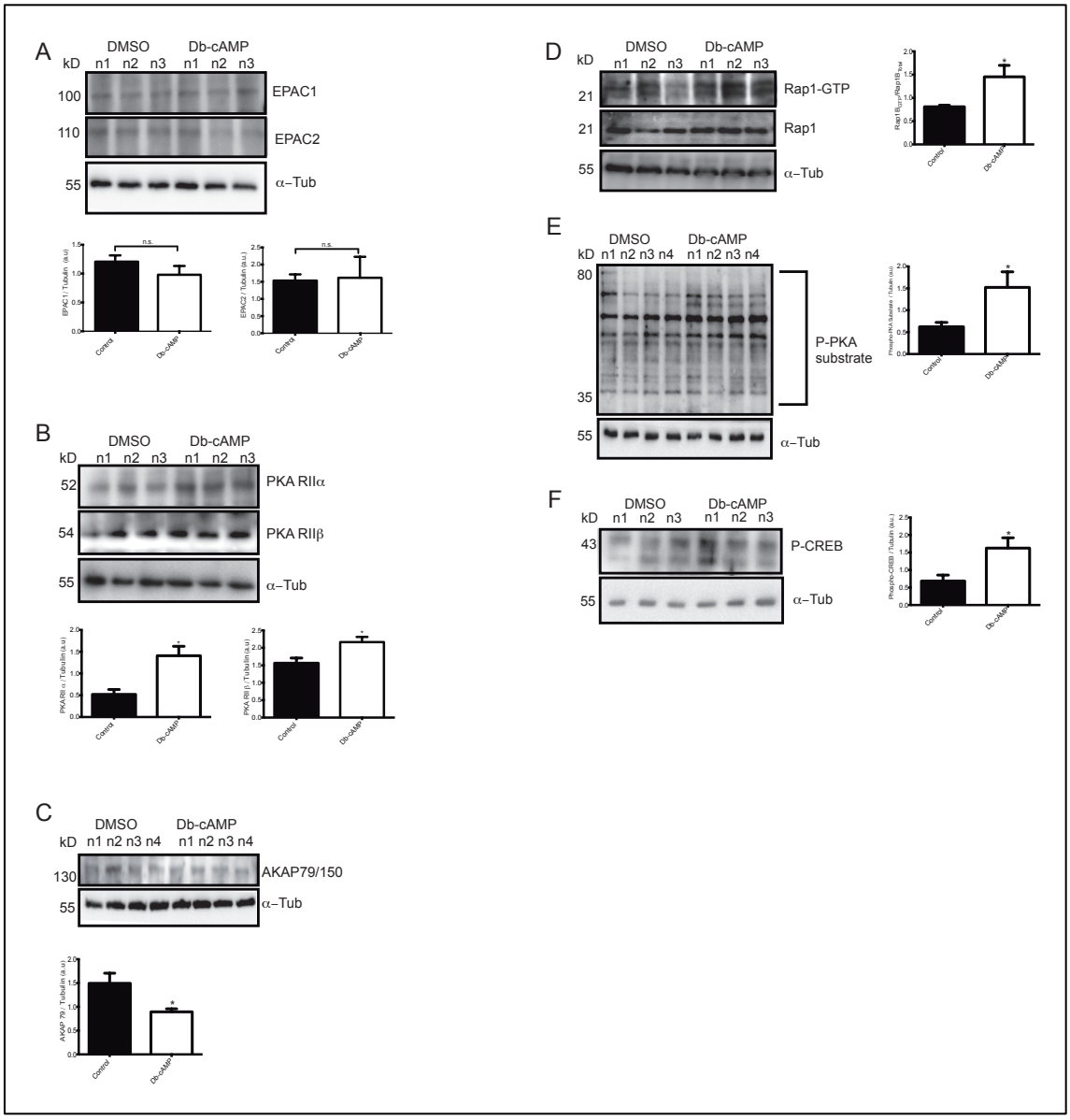
A
DMSO
Db-cAMP
kD
n1 n2 n3 n1 n2 n3
100
110
55
EPAC1
EPAC2
α–Tub
n.s.
Control
Db-cAMP
B
52
54
PKA RIIα
PKA RIIβ
C
n1 n2 n3 n4
130
AKAP79/150
D
21
Rap1-GTP
Rap1
E
80
35
P-PKA substrate
F
43
P-CREB

Figure 4

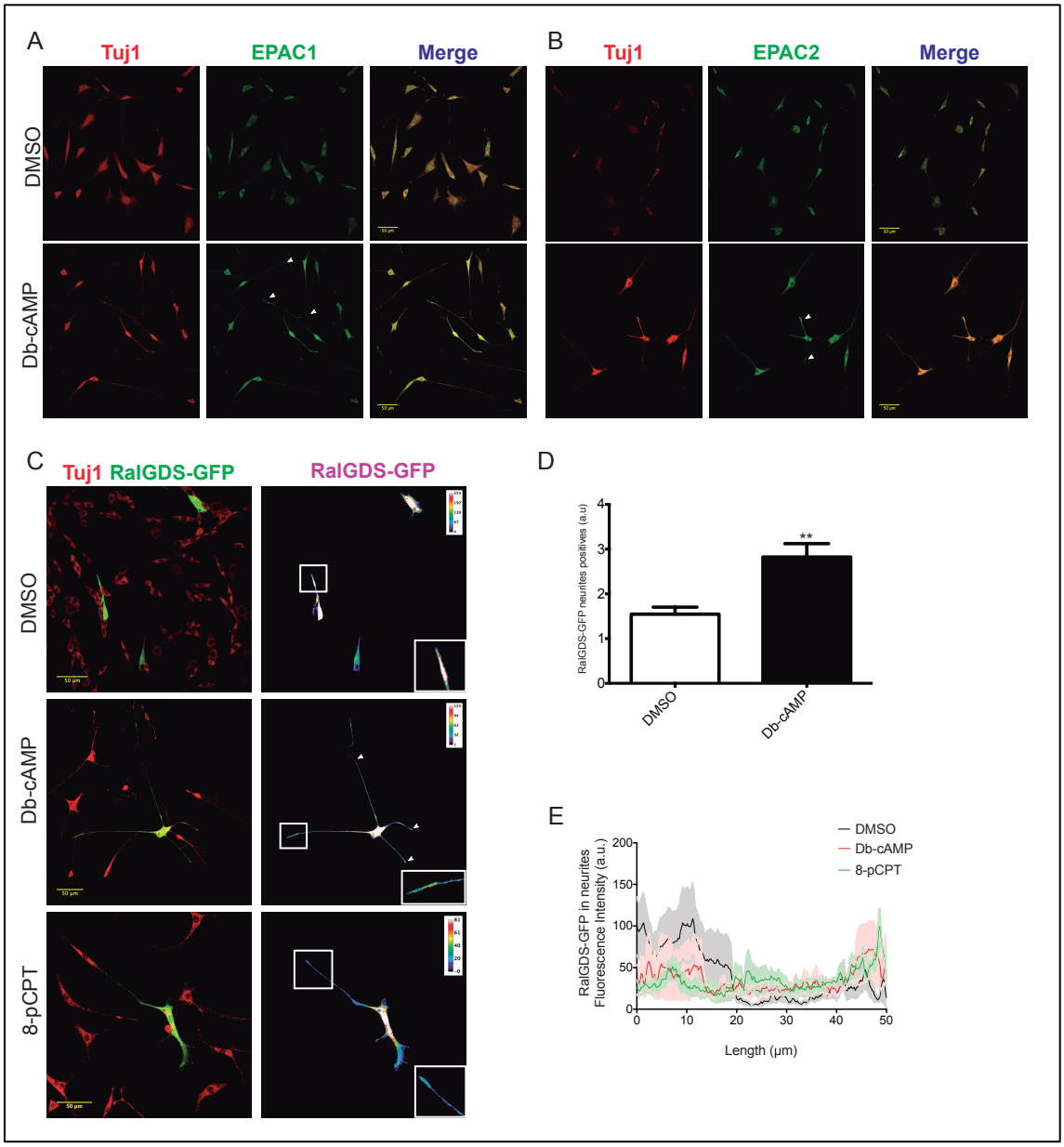
A
Tuj1
EPAC1
Merge
DMSO
Db-cAMP
B
Tuj1
EPAC2
Merge
C
Tuj1 RalGDS-GFP
RalGDS-GFP
DMSO
Db-cAMP
8-pCPT
D
RalGDS-GFP neurites positives (a.u)
**
DMSO
Db-cAMP
E
DMSO
Db-cAMP
8-pCPT
RalGDS-GFP in neurites
Fluorescence Intensity (a.u.)
Length (µm)

Figure 5

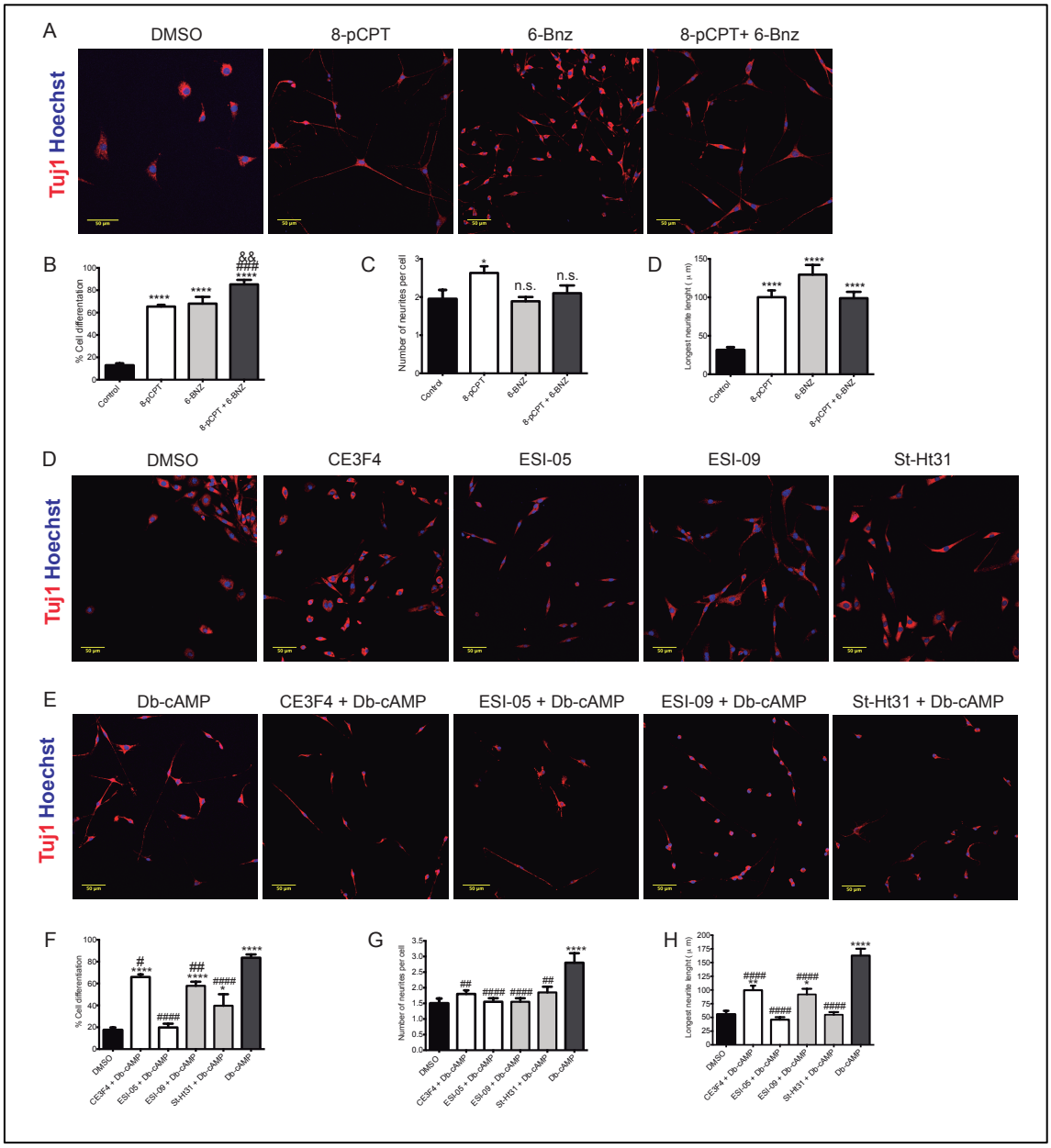
A
DMSO
8-pCPT
6-Bnz
8-pCPT+ 6-Bnz
Tuj1 Hoechst
B
% Cell differentiation
Control
8-pCPT
6-BNZ
8-pCPT + 6-BNZ
C
Number of neurites per cell
n.s.
n.s.
D
Longest neurite lenght (µ m)
D
DMSO
CE3F4
ESI-05
ESI-09
St-Ht31
Tuj1 Hoechst
E
Db-cAMP
CE3F4 + Db-cAMP
ESI-05 + Db-cAMP
ESI-09 + Db-cAMP
St-Ht31 + Db-cAMP
Tuj1 Hoechst
F
% Cell differentiation
DMSO
CE3F4 + Db-cAMP
ESI-05 + Db-cAMP
ESI-09 + Db-cAMP
St-Ht31 + Db-cAMP
Db-cAMP
G
Number of neurites per cell
H
Longest neurite lenght (µ m)

References

1. Banker GA, Cowan WM. Rat hippocampal neurons in dispersed cell culture. Brain Res. 1977;126(3):397-42.
2. Dotti CG, Sullivan CA, Banker GA. The establishment of polarity by hippocampal neurons in culture. J Neurosci. 1988;8(4):1454-68.
3. Greene LA, Tischler AS. Establishment of a noradrenergic clonal line of rat adrenal pheochromocytoma cells which respond to nerve growth factor. Proc Natl Acad Sci U S A. 1976;73(7):2424-8.
4. Encinas M, Iglesias M, Liu Y, Wang H, Muhaisen A, Cena V, et al. Sequential treatment of SH-SY5Y cells with retinoic acid and brain-derived neurotrophic factor gives rise to fully differentiated, neurotrophic factor-dependent, human neuron-like cells. Journal of neurochemistry. 2000;75(3):991-1003.
5. Tremblay RG, Sikorska M, Sandhu JK, Lanthier P, Ribecco-Lutkiewicz M, Bani-Yaghoub M. Differentiation of mouse Neuro 2A cells into dopamine neurons. Journal of neuroscience methods. 2010;186(1):60-7.
6. Amano T, Richelson E, Nirenberg M. Neurotransmitter synthesis by neuroblastoma clones (neuroblast differentiation-cell culture-choline acetyltransferase-acetylcholinesterase-tyrosine hydroxylase-axons-dendrites). Proc Natl Acad Sci U S A. 1972;69(1):258-63.
7. Kato H, Kato T, Sakazaki Y, Yamakawa Y, Naganawa N, Funabiki J, et al. Potentiation by BL191 of differentiation of neuroblastoma cells induced by dibutyryl cAMP and prostaglandin E(1). Neurochemistry international. 1982;4(5):419-26.
8. Shelly M, Lim BK, Cancedda L, Heilshorn SC, Gao H, Poo MM. Local and long-range reciprocal regulation of cAMP and cGMP in axon/dendrite formation. Science. 2010;327(5965):547-52.
9. de Rooij J, Zwartkruis FJ, Verheijen MH, Cool RH, Nijman SM, Wittinghofer A, et al. EPAC is a Rap1 guanine-nucleotide-exchange factor directly activated by cyclic AMP. Nature. 1998;396(6710):474-7.
10. Dao KK, Teigen K, Kopperud R, Hodneland E, Schwede F, Christensen AE, et al. EPAC1 and cAMP-dependent protein kinase holoenzyme have similar cAMP affinity, but their cAMP domains have distinct structural features and cyclic nucleotide recognition. J Biol Chem. 2006;281(30):21500-11.
11. Reagan LP, Ye XH, Mir R, DePalo LR, Fluharty SJ. Up-regulation of angiotensin II receptors by in vitro differentiation of murine N1E-115 neuroblastoma cells. Mol Pharmacol. 1990;38(6):878-86.
12. Oh JE, Karlmark Raja K, Shin JH, Pollak A, Hengstschlager M, Lubec G. Cytoskeleton changes following differentiation of N1E-115 neuroblastoma cell line. Amino acids. 2006;31(3):289-98.
13. Kiermayer S, Biondi RM, Imig J, Plotz G, Haupenthal J, Zeuzem S, et al. EPAC activation converts cAMP from a proliferative into a differentiation signal in PC12 cells. Mol Biol Cell. 2005;16(12):5639-48.
14. Sanchez S, Jimenez C, Carrera AC, Diaz-Nido J, Avila J, Wandosell F. A cAMP-activated pathway, including PKA and PI3K, regulates neuronal differentiation. Neurochemistry international. 2004;44(4):231-42.

15. Luskin MB, Parnavelas JG, Barfield JA. Neurons, astrocytes, and oligodendrocytes of the rat cerebral cortex originate from seParate progenitor cells: an ultrastructural analysis of clonally related cells. J Neurosci. 1993;13(4):1730-50.
16. Nakamuta S, Funahashi Y, Namba T, Arimura N, Picciotto MR, Tokumitsu H, et al. Local application of neurotrophins specifies axons through inositol 1,4,5-trisphosphate, calcium, and Ca2+/calmodulin-dependent protein kinases. Science signaling. 2011;4(199):ra76.
17. Mandell JW, Banker GA. A spatial gradient of tau protein phosphorylation in nascent axons. J Neurosci. 1996;16(18):5727-40.
18. Gonzalez-Billault C, Avila J, Caceres A. Evidence for the role of MAP1B in axon formation. Mol Biol Cell. 2001;12(7):2087-98.
19. Arimura N, Menager C, Fukata Y, Kaibuchi K. Role of CRMP-2 in neuronal polarity. J Neurobiol. 2004;58(1):34-47.
20. Henriquez DR, Bodaleo FJ, Montenegro-Venegas C, Gonzalez-Billault C. The light chain 1 subunit of the microtubule-associated protein 1B (MAP1B) is responsible for Tiam1 binding and Rac1 activation in neuronal cells. PLoS One. 2012;7(12):e53123.
21. Liu AY, Kamalakannan V, Chen KY. Identification of functional cAMP-dependent protein kinase in a 'neurite minus' mouse neuroblastoma cell line. Biochim Biophys Acta. 1987;928(2):235-9.
22. Witte H, Neukirchen D, Bradke F. Microtubule stabilization specifies initial neuronal polarization. J Cell Biol. 2008;180(3):619-32.
23. Janke C, Kneussel M. Tubulin post-translational modifications: encoding functions on the neuronal microtubule cytoskeleton. Trends in neurosciences. 2010;33(8):362-72.
24. Gonzalez-Billault C, Engelke M, Jimenez-Mateos EM, Wandosell F, Caceres A, Avila J. Participation of structural microtubule-associated proteins (MAPs) in the development of neuronal polarity. J Neurosci Res. 2002;67(6):713-9.
25. Conde C, Caceres A. Microtubule assembly, organization and dynamics in axons and dendrites. Nat Rev Neurosci. 2009;10(5):319-32.
26. Cravchik A, Reddy D, Matus A. Identification of a novel microtubule-binding domain in microtubule-associated protein 1A (MAP1A). Journal of cell science. 1994;107 (Pt 3):661-72.
27. Grabham PW, Seale GE, Bennecib M, Goldberg DJ, Vallee RB. Cytoplasmic dynein and LIS1 are required for microtubule advance during growth cone remodeling and fast axonal outgrowth. J Neurosci. 2007;27(21):5823-34.
28. Fukata Y, Itoh TJ, Kimura T, Menager C, Nishimura T, Shiromizu T, et al. CRMP-2 binds to tubulin heterodimers to promote microtubule assembly. Nature cell biology. 2002;4(8):583-91.
29. Morii H, Shiraishi-Yamaguchi Y, Mori N. SCG10, a microtubule destabilizing factor, stimulates the neurite outgrowth by modulating microtubule dynamics in rat hippocampal primary cultured neurons. J Neurobiol. 2006;66(10):1101-14.

30. Cheng X, Ji Z, Tsalkova T, Mei F. EPAC and PKA: a tale of two intracellular cAMP receptors. Acta Biochim Biophys Sin (Shanghai). 2008;40(7):651-62.
31. Birkeland E, Nygaard G, Oveland E, Mjaavatten O, Ljones M, Doskeland SO, et al. EPAC-induced Alterations in the Proteome of Human SH-SY5Y Neuroblastoma Cells. Journal of Proteomics & Bioinformatics. 2009;02(06):244-54.
32. Zhong H, Sia GM, Sato TR, Gray NW, Mao T, Khuchua Z, et al. Subcellular dynamics of type II PKA in neurons. Neuron. 2009;62(3):363-74.
33. Cadd GG, Uhler MD, McKnight GS. Holoenzymes of cAMP-dependent protein kinase containing the neural form of type I regulatory subunit have an increased sensitivity to cyclic nucleotides. J Biol Chem. 1990;265(32):19502-6.
34. Lohmann SM, Schwoch G, Reiser G, Port R, Walter U. Dibutyryl cAMP treatment of neuroblastoma-glioma hybrid cells results in selective increase in cAMP-receptor protein (R-I) as measured by monospecific antibodies. EMBO J. 1983;2(2):153-9.
35. Harada A, Teng J, Takei Y, Oguchi K, Hirokawa N. MAP2 is required for dendrite elongation, PKA anchoring in dendrites, and proper PKA signal transduction. J Cell Biol. 2002;158(3):541-9.
36. Glantz SB, Amat JA, Rubin CS. cAMP signaling in neurons: patterns of neuronal expression and intracellular localization for a novel protein, AKAP 150, that anchors the regulatory subunit of cAMP-dependent protein kinase II beta. Mol Biol Cell. 1992;3(11):1215-28.
37. Nijholt IM, Dolga AM, Ostroveanu A, Luiten PG, Schmidt M, Eisel UL. Neuronal AKAP150 coordinates PKA and EPAC-mediated PKB/Akt phosphorylation. Cell Signal. 2008;20(10):1715-24.
38. Bivona TG, Wiener HH, Ahearn IM, Silletti J, Chiu VK, Philips MR. Rap1 up-regulation and activation on plasma membrane regulates T cell adhesion. J Cell Biol. 2004;164(3):461-70.
39. Kortholt A, Bolourani P, Rehmann H, Keizer-Gunnink I, Weeks G, Wittinghofer A, et al. A Rap/phosphatidylinositol 3-kinase pathway controls pseudopod formation [corrected]. Mol Biol Cell. 2010;21(6):936-45.
40. Schwamborn JC, Puschel AW. The sequential activity of the GTPases Rap1B and Cdc42 determines neuronal polarity. Nat Neurosci. 2004;7(9):923-9.
41. Enserink JM, Christensen AE, de Rooij J, van Triest M, Schwede F, Genieser HG, et al. A novel EPAC-specific cAMP analogue demonstrates independent regulation of Rap1 and ERK. Nature cell biology. 2002;4(11):901-6.
42. Christensen AE, Selheim F, de Rooij J, Dremier S, Schwede F, Dao KK, et al. cAMP analog mapping of EPAC1 and cAMP kinase. Discriminating analogs demonstrate that EPAC and cAMP kinase act synergistically to promote PC-12 cell neurite extension. J Biol Chem. 2003;278(37):35394-402.
43. Courilleau D, Bouyssou P, Fischmeister R, Lezoualc'h F, Blondeau JP. The (R)-enantiomer of CE3F4 is a preferential inhibitor of human exchange protein directly activated by cyclic AMP isoform 1 (EPAC1). Biochemical and biophysical research communications. 2013;440(3):443-8.

44. Almahariq M, Tsalkova T, Mei FC, Chen H, Zhou J, Sastry SK, et al. A novel EPAC-specific inhibitor suppresses pancreatic cancer cell migration and invasion. Mol Pharmacol. 2013;83(1):122-8.
45. Tsalkova T, Mei FC, Li S, Chepurny OG, Leech CA, Liu T, et al. Isoform-specific antagonists of exchange proteins directly activated by cAMP. Proc Natl Acad Sci U S A. 2012;109(45):18613-8.
46. Poppinga WJ, Heijink IH, Holtzer LJ, Skroblin P, Klussmann E, Halayko AJ, et al. A-kinase-anchoring proteins coordinate inflammatory responses to cigarette smoke in airway smooth muscle. American journal of physiology Lung cellular and molecular physiology. 2015;308(8):L766-75.
47. Schmidt M, Dekker FJ, Maarsingh H. Exchange protein directly activated by cAMP (EPAC): a multidomain cAMP mediator in the regulation of diverse biological functions. Pharmacological reviews. 2013;65(2):670-709.
48. Oh JE, Karlmark KR, Shin JH, Pollak A, Freilinger A, Hengstschlager M, et al. Differentiation of neuroblastoma cell line N1E-115 involves several signaling cascades. Neurochemical research. 2005;30(3):333-48.
49. Oh JE, Freilinger A, Gelpi E, Pollak A, Hengstschlager M, Lubec G. Proteins involved in neuronal differentiation of neuroblastoma cell line N1E-115. Electrophoresis. 2007;28(12):2009-17.
50. Cosgrove C, Cobbett P. Induction of temporally dissociated morphological and physiological differentiation of N1E-115 cells. Brain Res Bull. 1991;27(1):53-8.
51. Busch C, Siegenthaler G, Vahlquist A, Nordlinder H, Sundelin J, Saksena P, et al. Expression of cellular retinoid-binding proteins during normal and abnormal epidermal differentiation. J Invest Dermatol. 1992;99(6):795-802.
52. Clejan S, Dotson RS, Wolf EW, Corb MP, Ide CF. Morphological differentiation of N1E-115 neuroblastoma cells by dimethyl sulfoxide activation of lipid second messengers. Exp Cell Res. 1996;224(1):16-27.
53. Kranenburg O, Scharnhorst V, Van der Eb AJ, Zantema A. Inhibition of cyclin-dependent kinase activity triggers neuronal differentiation of mouse neuroblastoma cells. J Cell Biol. 1995;131(1):227-34.
54. Erck C, Peris L, Andrieux A, Meissirel C, Gruber AD, Vernet M, et al. A vital role of tubulin-tyrosine-ligase for neuronal organization. Proc Natl Acad Sci U S A. 2005;102(22):7853-8.
55. Utreras E, Jimenez-Mateos EM, Contreras-Vallejos E, Tortosa E, Perez M, Rojas S, et al. Microtubule-associated protein 1B interaction with tubulin tyrosine ligase contributes to the control of microtubule tyrosination. Dev Neurosci. 2008;30(1-3):200-10.
56. Shea TB, Beermann ML, Nixon RA. Post-translational modification of alpha-tubulin by acetylation and detyrosination in NB2a/d1 neuroblastoma cells. Brain Res Dev Brain Res. 1990;51(2):195-204.
57. DiTella MC, Feiguin F, Carri N, Kosik KS, Caceres A. MAP-1B/TAU functional redundancy during laminin-enhanced axonal growth. Journal of cell science. 1996;109 (Pt 2):467-77.
58. Bielas S, Higginbotham H, Koizumi H, Tanaka T, Gleeson JG. Cortical neuronal migration mutants suggest seParate but intersecting pathways. Annu Rev Cell Dev Biol. 2004;20:593-618.

59. Messi E, Florian MC, Caccia C, Zanisi M, Maggi R. Retinoic acid reduces human neuroblastoma cell migration and invasiveness: effects on DCX, LIS1, neurofilaments-68 and vimentin expression. BMC Cancer. 2008;8:30.
60. Inagaki N, Chihara K, Arimura N, Menager C, Kawano Y, Matsuo N, et al. CRMP-2 induces axons in cultured hippocampal neurons. Nat Neurosci. 2001;4(8):781-2.
61. Cheng PL, Lu H, Shelly M, Gao H, Poo MM. Phosphorylation of E3 ligase Smurf1 switches its substrate preference in support of axon development. Neuron. 2011;69(2):231-43.
62. Marler KJ, Kozma R, Ahmed S, Dong JM, Hall C, Lim L. Outgrowth of neurites from NIE-115 neuroblastoma cells is prevented on repulsive substrates through the action of PAK. Mol Cell Biol. 2005;25(12):5226-41.
63. Huang YA, Kao JW, Tseng DT, Chen WS, Chiang MH, Hwang E. Microtubule-associated type II protein kinase A is important for neurite elongation. PLoS One. 2013;8(8):e73890.
64. Grandoch M, Roscioni S, Schmidt M. The role of EPAC proteins, novel cAMP mediators, in the regulation of immune, lung and neuronal function. British journal of pharmacology. 2010;159(2):265-84.
65. Hochbaum D, Tanos T, Ribeiro-Neto F, Altschuler D, Coso OA. Activation of JNK by EPAC is independent of its activity as a Rap guanine nucleotide exchanger. J Biol Chem. 2003;278(36):33738-46.
66. Shi GX, Rehmann H, Andres DA. A novel cyclic AMP-dependent EPAC-Rit signaling pathway contributes to PACAP38-mediated neuronal differentiation. Mol Cell Biol. 2006;26(23):9136-47.
67. Li Y, Asuri S, Rebhun JF, Castro AF, Paranavitana NC, Quilliam LA. The RAP1 guanine nucleotide exchange factor EPAC2 couples cyclic AMP and Ras signals at the plasma membrane. J Biol Chem. 2006;281(5):2506-14.
68. Moon MY, Kim HJ, Kim JG, Lee JY, Kim J, Kim SC, et al. Small GTPase Rap1 regulates cell migration through regulation of small GTPase RhoA activity in response to transforming growth factor-beta1. J Cell Physiol. 2013;228(11):2119-26.
69. Muñoz-Llancao P HD, Wilson C, Bodaleo F, Boddeke E, Schmidt M, González-Billault C. Exchange protein directly activated by cAMP (EPAC) regulates neuronal polarization through Rap1B. J Neurosci2015.
70. Murray AJ, Shewan DA. EPAC mediates cyclic AMP-dependent axon growth, guidance and regeneration. Mol Cell Neurosci. 2008;38(4):578-88.
71. Srivastava DP, Woolfrey KM, Jones KA, Anderson CT, Smith KR, Russell TA, et al. An autism-associated variant of EPAC2 reveals a role for Ras/EPAC2 signaling in controlling basal dendrite maintenance in mice. PLoS Biol. 2012;10(6):e1001350.
72. Tunquist BJ, Hoshi N, Guire ES, Zhang F, Mullendorff K, Langeberg LK, et al. Loss of AKAP150 perturbs distinct neuronal processes in mice. Proc Natl Acad Sci U S A. 2008;105(34):12557-62.
73. Wang Y, Chen Y, Chen M, Xu W. AKAPs competing peptide HT31 disrupts the inhibitory effect of PKA on RhoA activity. Oncol Rep. 2006;16(4):755-61.